Phosphodiesterase-8A binds to and regulates Raf-1 kinase

Kim M. Brown[C], Jon P. Day[C], Elaine Huston[C], Bastian Zimmermann[$], Kornelia Hampel,[$], Frank Christian[C,]., David Romano[a], Selim Terhzaz[D], Louisa C. Y. Lee[C], Miranda J. Willis[C], David B. Morton[&], Joseph A. Beavo[^], Masami Shimizu-Albergine[^], Shireen A. Davies[D], Walter Kolch[a,b], Miles D. Houslay*, George S. Baillie[C]

[a] Systems Biology Ireland, University College Dublin, Dublin 4, Ireland [b] Conway Institute of Biomolecular & Biomedical Research, University College Dublin, Dublin 4, Ireland [C]Institute of Cardiovascular and Medical Science, College of Medical, Veterinary and Life Sciences, University of Glasgow, Glasgow G12 8QQ, Scotland, UK [D]Institute of Molecular, Cellular and Systems Biology, College of Medical, Veterinary and Life Sciences, University of Glasgow, Glasgow G12 8QQ, Scotland, UK [$]Biaffin GmbH & Co KG, Heinrich-Plett-Strasse 40, 34132 Kassel, Germany [&]Department of Integrative Biosciences, 611 SW Campus Drive, Oregon Health Science University, Portland, Oregon 97239. USA [^]Department of Pharmacology, University of Washington, Seattle, Washington 98159. USA *Institute of Pharmaceutical Sciences, King's College, 150 Stamford Street, London. SE1 9NH. UK

Raf-1 is a key activator of the Extracellular signal Regulated Kinase (ERK) pathway and a target for cross-regulation of this pathway by the cAMP signalling system. The cAMP activated protein kinase (PKA) inhibits Raf-1 by phosphorylation on S259. Here, we show that the cAMP-degrading phosphodiesterase-8A (PDE8A) associates with Raf-1 to protect it from inhibitory phosphorylation by PKA, thereby enhancing Raf-1's ability to stimulate ERK signalling. PDE8A binds to Raf-1 with high (picomolar) affinity. Mapping of the interaction domain on PDE8A using peptide array technology identified amino acids 454-465 as the main binding site, which could be disrupted by mutation. A cell permeable peptide corresponding to this region, disrupted the PDE8A/Raf-1 interaction in cells, thereby reducing ERK activation and the cellular response to EGF. Overexpression of a catalytically inactive PDE8A in cells displayed a dominant negative phenotype on ERK activation. These effects were recapitulated at the organism level in genetically modified mice (PDE8A -/-) that lack PDE8A. Similarly, PDE8 deletion in Drosophila melanogaster also reduced basal ERK activation and sensitized flies to stress-induced death. We propose that PDE8A is a novel physiological regulator of Raf-1 signalling in some cells.

cAMP | map kinase | PDE | phosphodiesterase | Raf-1

INTRODUCTION

Raf-1 is at the apex of the MEK-ERK pathway, which controls many fundamental biological processes including cell proliferation, survival and transformation. In this pathway Raf-1 phosphorylates and activates MEK, which in turn phosphorylates and activates ERK. ERK has more than 150 known substrates, which mediate many of the pleiotropic functions of this pathway (1). Raf-1 regulation is complex and still insufficiently understood. Critical events are the dephosphorylation of an inhibitory site, S259, which allows Raf-1 binding to activated Ras and is a prerequisite for further activation (2, 3). S259 is a target for phosphorylation by PKA (4, 5) and is part of a complex system of crosstalk between the cAMP and the ERK pathways.

The cAMP system is the first signal transduction system discovered mediating the intracellular biochemical effects of hormones (6), and PKA has been recognised as a main effector of cAMP (7). The intimate connections between the cAMP and ERK pathways were first revealed when PKA was shown to inhibit Raf-1 by direct phosphorylation (8-13). The exact mechanism of inhibition has remained unclear. Several phosphorylation sites in Raf-1 were invoked in the inhibitory action, e.g. S43 which could interfere with Raf-1 binding to Ras (13), S621 which can directly inhibit Raf-1 kinase activity (10), S233 which mediates inhibitory14-3-3 binding and S259 which blocks Raf-1 translocation to the plasma membrane and Ras binding (4, 5). While the mechanistic function of most of these phosphorylation sites has remained controversial (14), S259 has emerged clearly as major inhibitory site, whose dephosphorylation is part of the physiological activation process of Raf-1 and is mandatory for Raf-1 activation to ensue (2, 3). In addition, several other mechanisms of crosstalk have been discovered including the regulation of Ras family proteins by cAMP sensitive exchange factors and the phosphorylation of phosphodiesterases (PDEs) by ERK (15, 16).

Cyclic nucleotide phosphodiesterases (PDEs) terminate cAMP signalling by hydrolysing cAMP, with this enzyme class featuring a large number of genes and isoforms that are regulated by differential expression, alternative splicing and distinct modes of subcellular compartmentalisation (17). Critically, studies on the cAMP specific phoshodiesterase-4 (PDE4) family of enzymes have shown that the targeting of distinct PDE isoforms to specific signalling complexes and localities in cells underpins compartmentalised cAMP signalling (18, 19). This allows for the development of spatially discrete gradients of cAMP that control spatially restricted sub-populations of the cAMP effectors, PKA and EPAC (20).

Recently, there has been a surge of interest in the cAMP specific phoshodiesterase-8 (PDE8) family of enzymes. PDE8s are expressed widely in human tissue (21) with functions in testosterone production (22), lymphocyte adhesion (23), chemotaxis (24) and excitation-contraction coupling in ventricular myocytes (25). PDE8 isoforms exhibit an extremely high affinity for cAMP (26) and this unique feature has led to the suggestion that PDE8

Significance

The extracellular signal regulated kinase (ERK) pathway is a ubiquitous mechanism for transducing a variety of extra cellular signals into intracellular events. It is also mis-regulated in a number of different disease states including several cancers. The ERK pathway crosstalks with other signaling cascades, including the cAMP system. In this paper, we show that a key component of the ERK pathway, Raf-1 kinase, can associate a specific cyclic nucleotide phosphodiesterase (PDE8A) to modulate the activity of the kinase. We report that the interaction between Raf-1 and PDE8A underpins functional consequences of ERK signaling in several different model systems.

Reserved for Publication Footnotes

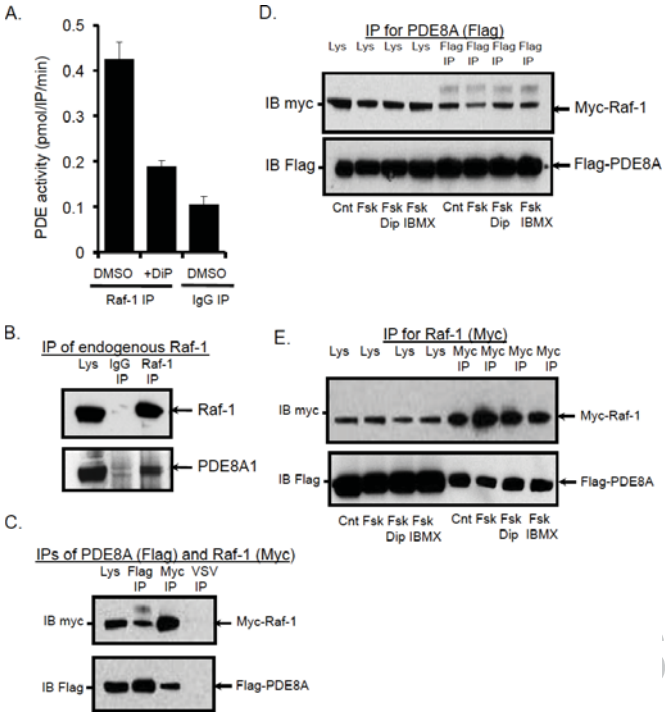

Fig. 1. – PDE8 and Raf-1 form a constitutively assembled complex. A. Immunoprecipitations of Raf-1 or control IgG from HeLa cells were analysed for associated PDE activity. Raf-1 Ips contained PDE activity that was inhibited by 100μM dipyridimole. B. Immunoprecipitates of endogenous Raf-1 from HeLA cells brings down PDE8A1. C. Tagged constructs of Raf-1 (Myc tag) and PDE8A (Flag tag) were co-expressed in HEK293 and immunoprecipitates (IPs) of both tags probed for both Myc-Raf-1 and Flag- PDE8A. D., IPs with PDE8A Flag antibody and E., IPs with Raf-1 Myc antibody. IPs as in A. were repeated following treatment with forskolin alone (100μM, 10 minutes) or with forskolin (100μM, 10 minutes) in conjunction with either a non-selective PDE inhibitor (IBMX, 100μM, 10 minutes pre-treatment) or a PDE8 selective inhibitor (dipyridimole, 100μM, 10 minutes pre-treatment).

enzymes may have a very important cellular role in protecting any associated protein from fluctuations in basal cAMP concentrations. Compartmentalisation of cAMP specific PDEs with PKA substrates has been recognised as a mechanism that not only protects the substrates from inappropriate PKA phosphorylation under basal conditions but also ensures specificity of action when a single receptor type is activated to produce a second messenger, such as cAMP, that is common to many other receptors (19). Here, we report that at least part of the PDE8A in the cell can bind tightly to Raf-1, regulate Raf-1 phosphorylation on S259 and, in so doing, regulate the cross-talk node whereby cAMP exerts an inhibitory effect on Raf-1 signalling through to ERK phosphorylation and activation.

RESULTS

PDE8A localises with Raf-1 immunoprecipitates.

To look for binding partners for Raf-1 immunoprecipitates of Raf-1 from HEK293 cells were digested with trypsin and subjected to peptide map finger printing analysis using a mass spectrometer. PDE8A was identified as a 95 kD Raf-1 associated protein with 7 PDE8A peptides identified in the spectra (suppl. Fig 1). To validate the interaction between Raf-1 and PDE8A, immunoprecipitates of Raf-1 were tested for PDE activity and were found to contain PDE activity that was inhibited by dipyridimole (DiP), an effective and partially selective PDE8 inhibitor (Fig. 1A). As this data strongly suggested that PDE8A and Raf-1 can exist in a complex, Raf-1 immunoprecipitates were screened for associated PDE8A using western blotting (Fig. 1B). Using

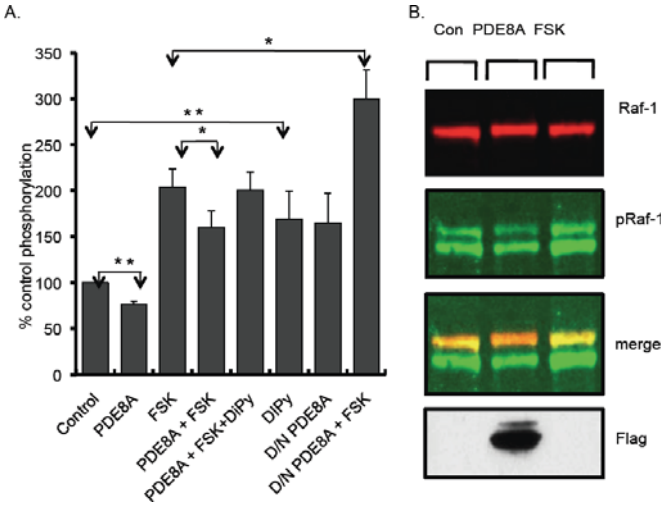

Fig. 2. – PDE8 activity regulates phosphorylation of Raf-1 at serine 259. A.HEK293 cells were transfected with Flag-PDE8A1 (lanes 2,4,5) or dominant negative PDE8A1 (lanes 7 and 8) and/or treated with dipyridamole (DiP, lanes 5 and 6) or forskolin (FSK, lanes 3,4,5 and 8). The level of phospho-Raf-1 (S259) relative to total Raf-1 was monitored using a Licor Odyssey® system, where the band density measured using a Raf-1 phospho-ser 259 antibody (upper band second top panel Fig. 2B) was divided by the total Raf-1 density (top panel Fig. 2B). Second bottom panel depicts the merged image of top and second top panel. B. Example data from Licor Odyssey®. Lower panel, western blot showing relative expression of PDE8A construct. Asterisks and p values shown are relative to the control sample unless otherwise indicated; n = 4, with the exception of the dominant negative PDE8A + forskolin sample where n = 3; * $p<0.05$; ** $p<0.01$.

this technique, a PDE8A specific antibody detected a protein of the correct weight that was associated with Raf-1. To further verify the association of Raf-1 and PDE8A, we undertook overexpression studies where epitope tagged constructs of Raf-1 (Myc tag) and PDE8A (Flag tag) were co-expressed in HEK293 cells and immunoprecipitates (IPs) of both tags were probed for both Myc-Raf-1 and Flag- PDE8A (Fig. 1C). Control immunoprecipitates used antibodies against an unrelated tag (VSV). Raf-1 co-immunoprecipitated with PDE8A and vice versa. The PDE8A – Raf-1 association was not due to non-specific interaction as the control IPs showed no co-immunoprecipitating species. To determine whether the association of PDE8A and Raf-1 depended on cAMP concentrations within cells, the immunoprecipitations were repeated following treatment with Forskolin alone or with Forskolin in conjunction with either a non-specific PDE inhibitor (IBMX) or a PDE8 selective inhibitor (Figs. 1D, E). None of these treatments influenced the amount of PDE8A that co-purified with Raf-1 or vice versa suggesting that a pre-formed complex of PDE8 and Raf-1 exists in HEK293 cells.

PDE8 activity regulates Raf-1 phosphorylation at Ser259

As the biochemical data above suggested an interaction between Raf-1 and PDE8A, we assessed whether PDE8 activity could influence the amount of basal phosphorylation of Raf-1 at serine 259 in HEK293 cells using Licor Odyssey® technology; a quantitative Western blotting method (Fig. 2). PDE8A over-expression significantly reduced phosphorylation at S259. Conversely, expression of a catalytically inactive form of PDE8A(D/N-PDE8A) resulted in a dominant negative phenotype, a concept developed previously by us in studies of PDE4 isoforms (McCahill et al, 2005). Overexpression of this type of construct significantly augmented phosphorylation at S259 on Raf1 presumably by displacing the endogenous PDE8A from its binding site on Raf-1 (Fig. 2). Treatment with the partially selective PDE8 inhibitor dipyridimole, also significantly increased S259 phosphorylation of Raf-1. Additionally, increases in Raf-1

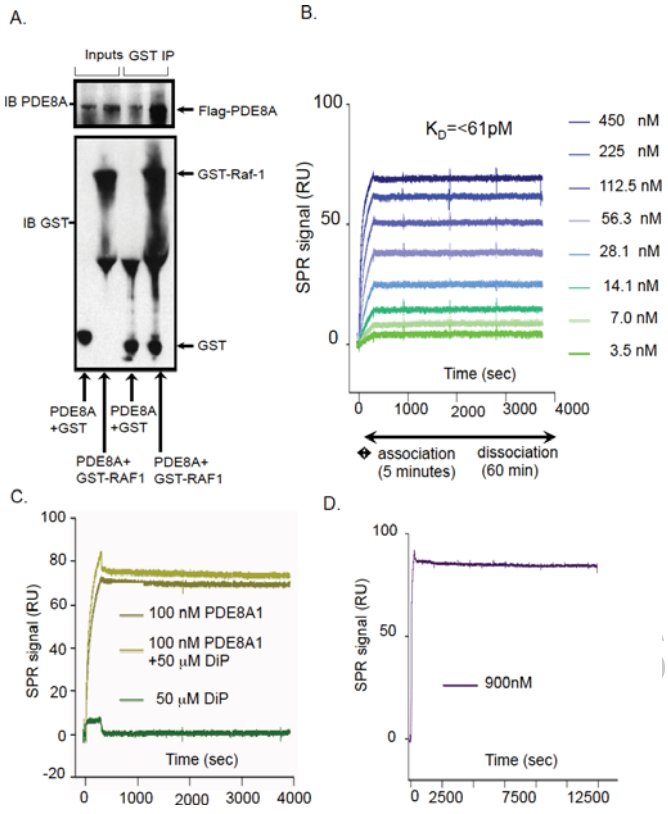

Fig. 3. – **PDE8A binds to Raf-1 with high affinity.** A. Purified PDE8-MBP was mixed with purified GST-Raf-1 or GST alone and a GST-pulldown experiment was undertaken (see methods). B. GST-Raf-1 was coupled to a biacore chip using an anti-GST antibody and probed with increasing concentrations of MBP-PDE8A. C. MBP-PDE8A (100nM) was used to probe a GST-Raf1 chip. The injection was done with or without inclusion of 50μM Dipyridimole. A control injection of 50μM Dipyridimole was also undertaken. D. Dissociation of the GST-Raf1-PDE8-MBP complex was observed over 250 minutes

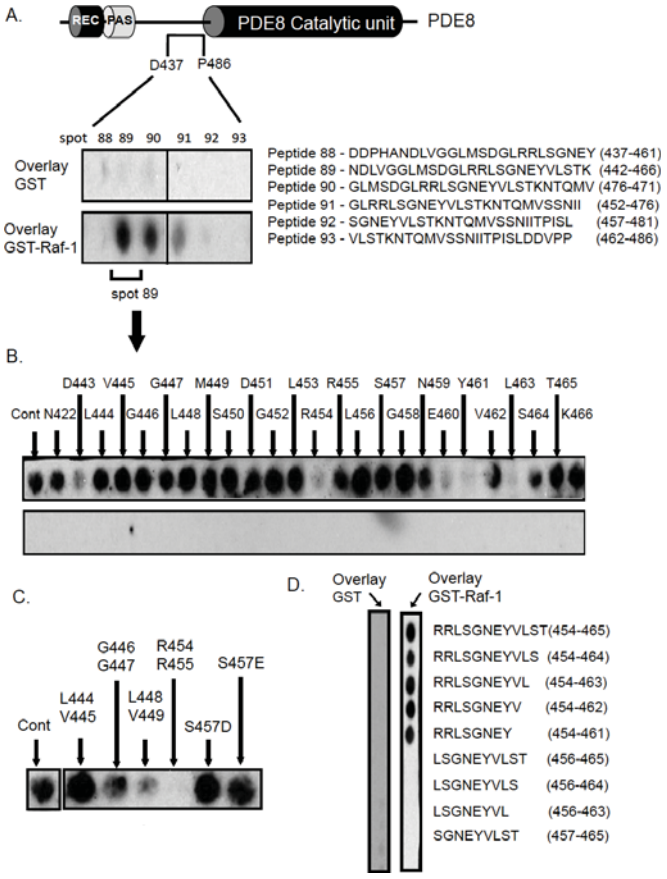

Fig. 4. – **Mapping of the Raf-1 binding site on PDE8A**. A. A peptide array of human PDE8A consisting of 25mer peptides overlapping by 5 amino acids that encompassed the entire PDE8A sequence was overlain with either GST or GST-Raf-1. Positive interactions were detected with peptides 89,90 and 91 that correspond to a sequence encompassing amino acids 442-476 of PDE8A1. B. Peptide arrays where successive residues of the sequence within peptide 89 (442-466) were substituted with alanine were overlain with either GST or GST-Raf-1. C. Stepwise C-terminal truncation of sequences within peptide 89 revealed the "core" binding motif that associates with Raf-1.

S259 phosphorylation that ensued upon treatment of cells with the adenylyl cyclase activator, forskolin, were either inhibited by PDE8A overexpression or augmented by D/N-PDE8A overexpression. As PDE8A activity makes up a small percentage of the total PDE activity in these cells (<5%) but has such a profound effect on basal phospho- S259 Raf-1 levels (Fig. 2, bars 6,7 and 8), but not the global PKA phosphorylation of PKA substrates (suppl. Fig. 2), we decided to ascertain whether PDE8A and Raf-1 interact directly.

PDE8A interacts directly with Raf-1.

In order to determine whether the interaction was direct, we incubated purified PDE8-MBP with either GST-Raf-1 or GST and performed a GST-pulldown experiment (Fig. 3A). PDE8 co-purified with GST-Raf-1 but not with GST alone, suggesting that the interaction between PDE8 and Raf-1 is direct. Finally, we determined the affinity of the interaction of PDE8A and Raf-1 via Surface Plasmon Resonance analysis (SPR) (Fig. 3B). GST-Raf-1 was coupled to the chip using an anti-GST antibody (see methods) and probed with MBP-PDE8A (Fig. 3B). The affinity of interaction was extremely high, being in the mid to low picomolar range (K_D < 61pM). However, as the affinity of the proteins was so high, less than 5% dissociation occurred during an extended assay time of 4 hours, thus precluding an accurate determination of the rate of dissociation (Fig. 3C). Therefore, the upper limit of k_d has been used for calculating the equilibrium dissociation constant K_D. We additionally tested the effects of dipyridimole on the formation and stability of the complex, but this inhibitor did not alter the interaction between Raf-1 and PDE8A (Fig. 3D). This indicates that inhibitor binding to the active site does not affect the interaction between PDE8 and Raf-1. Control chips that had reference surfaces consisting of immobilised GST alone showed no interaction with MBP-PDE8A.

Mapping the site of interaction for Raf-1 on PDE8A

Peptide array technology has been successfully used by us (27-29) and others (30, 31) to map the interfaces between interacting proteins. This information can be used to design cell-permeable disrupting peptides and to inform mutagenesis strategies aimed at creating null binding mutants (32, 33). In order to map the sites of interaction between Raf-1 and PDE8A, we synthesised a peptide array of human PDE8A consisting of 25mer peptides overlapping by 5 amino acids that encompassed the entire PDE8A sequence (Fig 4). We then probed this array with either GST or GST-Raf-1 and detected areas of interaction by blotting for the GST tag. A robust interaction of GST-Raf-1 (but not GST alone) was identified on peptide spots 89, 90 and 91, which correspond to amino acids 442 – 476 within the PDE8A sequence (Fig. 4A). A detailed alanine scan of this region, where successive residues were substituted with alanine residues, showed that the major residues involved in the interaction were D443, R454, R455, E460, Y461 and L463 (Fig. 4B). Further proof that the PDE8A sequence 454-461 (RRLSGNEY) was required for the association of Raf-1 was obtained using truncation analysis (Fig 4C) of immobilised peptides. Stepwise C-terminal truncation revealed

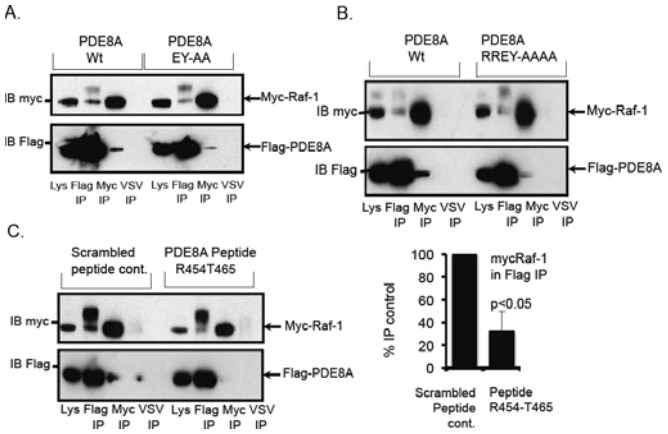

Fig. 5. Dissociation of the PDE8A-Raf-1 complex by site directed mutagenesis and peptide disruption. A. Mutation of PDE8A1 residues $^{460}E^{461}Y$ to alanines attenuated the interaction between PDE8A and Raf-1 as measured by co-immunoprecipitation. B. Quadruple mutation of PDE8A1 residues $^{454}R^{455}R^{460}E^{461}Y$ to alanine further attenuated the interaction between PDE8A and Raf-1 as measured by co-immunoprecipitation. C. A cell-permeable peptide corresponding to amino acids R454-T465 attenuated the association between PDE8A and Raf-1 when measured in immunoprecipitation experiments from cellular lysates. A randomly scrambled version of this peptide (Scrambled peptide control) did not affect the interaction between PDE8A and Raf-1. D. Quantification of the effectiveness of the PDE8-Raf-1 disruptor peptide in dissociating the complex.

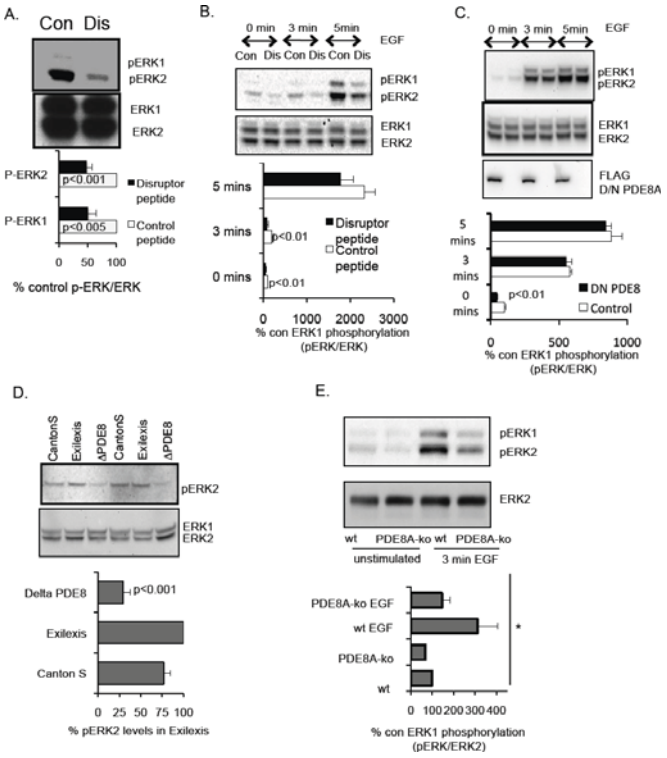

Fig. 6. - Manipulation of the PDE8 – Raf-1 complex alters the strength of basal and EGF stimulated phospho-ERK signals. A. Treatment of HEK293 cells with the disruptor peptide significantly down regulated basal phospho-ERK Map kinase levels compared to cells treated with the scrambled peptide control. n=3 B. Pre-treatment of HEK293 cells with disruptor peptide (Dis) (but not scrambled control (Cont)) significantly attenuated phospho-ERK levels induced by short term (0-3 minutes) EGF treatment. C. Over-expression of D/N PDE8 significantly reduced resting phospho-ERK levels in HEK293 cells. D. Basal phospho-ERK levels are significantly decreased in the PDE8 knock-out Drosophila when compared with two control lines. E. Basal phospho-ERK levels and those induced by short term (0-3 minutes) EGF treatment are attenuated in primary mouse Leydig cells derived from the PDE8A (-/-) mouse compared with those derived from a wild type mouse. n = 3, statistical analysis by 1-way ANOVA, * = significantly different with P = 0.037.

that this sequence was the minimum required to maintain Raf-1 binding.

To confirm the importance of PDE8A residues E460 and Y461 for the association of Raf-1, we mutated both residues to alanine and repeated the immunoprecipitation experiment from Fig 1. Mutation of these residues attenuated, but did not fully ablate, the interaction of the proteins (Fig. 5A), suggesting that other residues in the 454-461 (RRLSGNEY) minimum-binding region were also important for the formation of Raf-1-PDE8A complex. As a double alanine substitution of R454A:R455A was found to abolish Raf-1 interaction on peptide array (Fig. 4B) we combined this double mutation with the E460A:Y461A mutation. This quadruple mutant (R454A:R455:A:E460A:Y461A) further reduced binding to some 15.3% (mean of n=3 S.E. 3.8%, $p<0.05$) of the wild type (Fig. 5B), underlining the importance of this region in conferring interaction between PDE8A and Raf-1.

Peptide disruption of the Raf-1-PDE8A complex

Previous work from our laboratory has shown that cell-permeable analogues of 25mer peptides identified in this manner often can be used to disrupt signalling complexes within cells thereby effecting specific functional outputs such as phosphorylation of the β_2-adrenergic receptor by PKA (32) and the phosphorylation of βarrestin by ERK MAPK (28). In this study, we utilised the Raf-1 docking sequence from PDE8A, encompassing residues R454-T465, to manufacture a stearylated, cell-permeable disruptor peptide. We also synthesised a scrambled version of the stearylated peptide that had the same net weight and charge as a control (Peptide Cont). Both peptides had a C-terminal stearate group that has been shown to allow transport across the cell membrane (28). The disruptor peptide, but not the control peptide, attenuated the association between PDE8A and Raf-1 when measured in immunoprecipitation experiments from cellular lysates (Fig. 5C, D). The disruption of the complex induced by the peptide (33.8% (mean n=3, SE 18.1, $p<0.05$) was not as marked as that of the quadruple mutant R454A:R455:A:E460A:Y461A (15.3%, mean of n=3 S.E. 3.8%, $p<0.05$, Fig. 5B) but this could be due to cell permeability and affinity issues, as although we have treated cells with a relatively high concentration of peptide (10μM), we have no way of accurately measuring the amount that reaches the cell cytoplasm. We did, however, detect a 43% decrease in association of the endogenous proteins in HEK293 cells following treatment with disruptor peptide (Suppl. Fig. 3B). It should be noted that, as the affinity of the interaction is extremely high (Fig 3), we may not expect to achieve a complete disruption of a pre-formed complex between Raf-1 and PDE8A using a peptide. However, the disruptor peptide markedly decreased basal phospho-ERK in HEK293 cells (Fig. 6A), and increased basal phospho-Raf1 levels (suppl. Fig. 3A) and could markedly attenuate phospho-ERK levels induced by short term (0 - 3 minutes) EGF treatment (Fig. 6B).

In agreement with these results, over-expression of a catalytically inactive form of PDE8A exerted a dominant negative action by significantly reducing resting phospho-ERK levels in HEK293 cells. However in this case, the EGF induced phospho-ERK response remained unaltered (Fig. 6C).

To determine whether or not the control of resting phospho-ERK levels by PDE8A activity occurs at the organismal level, we studied the phospho-ERK levels in wild type fly strains that are known to exhibit canonical ERK signalling (34) and a PDE8 knock-out (PDE8 -/-) Drosophila mutant (Fig. 6D). We also determined phospho-ERK levels in the Leydig cells of an established PDE8A (PDE8A -/-) knock-out mouse model and compared them to levels observed in matched wild type controls (Fig. 6E). In agreement with the changes in basal phospho-ERK

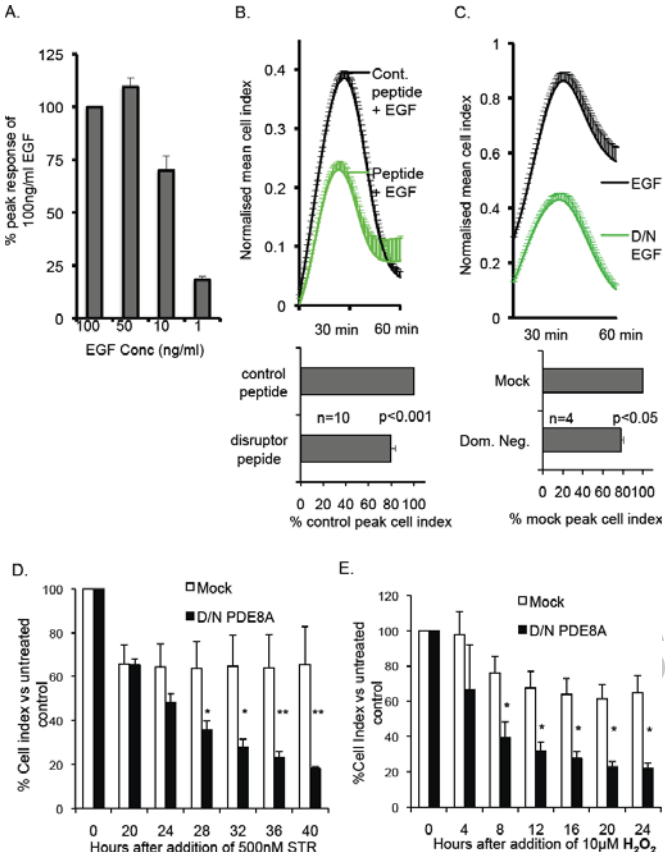

Fig. 7. - Disruption of the PDE8 – Raf-1 complex alters functional responses to EGF and stress signals. A. The EGF induced cell shape change in HeLa cells measured by real-time impedence measurement is dose dependent. B. The PDE8-Raf-1 disruptor peptide but not the scrambled control attenuates cell shape change induced by EGF in HeLa cells. C. Over-expression of D/N PDE8A significantly reduced cell shape changes in HeLa cells induced by EGF. D. Cell death in HEK293 cells induced by staurosporin (500 nM) treatment is enhanced when cells are transfected with D/N PDE8A. E. Cell death induced by hydrogen peroxide treatment (10μM) in HEK293 cells is enhanced when cells are transfected with D/N PDE8. *p<0.05, **p<0.01

seen HEK293 cells, resting phospho-ERK levels were markedly reduced in the both the PDE8 KO fly and PDE8A KO mouse. Phospho-ERK levels induced by 3 minutes EGF treatment were also significantly reduced in PDE8A KO mouse Leydig cells when compared with the same cells isolated from wild type mice (Fig. 6E).

Disruption of the PDE8A – Raf-1 complex alters functional responses to EGF and stress signals

Growth factor induced morphological changes can be quantified in cells by measuring impedance (35, 36) as this provides a real-time, non-invasive analysis suitable for measuring the kinetics of short and long-term cellular responses. Changes in cellular impedance triggered by agents such as EGF and insulin have been shown to correlate with those measured by conventional means, for example, autophosphorylation of the EGF receptor as measured by ELISA (35) and impedance is now commonly used for assessing morphological changes in a quantitative fashion such as membrane ruffling or formation of lamellipodia. We employed xCELLigence® technology (Roche) to measure the impedance of cell cultures in which we perturbed the PDE8A-Raf-1 interaction.

Firstly, to ensure a maximal signal we constructed a dose response curve in HeLa cells to evaluate the effect of increasing EGF concentration on cell impedance (Fig. 7A; "cell index"). Maximal response occurred at 50ng/ml EGF, a value reported

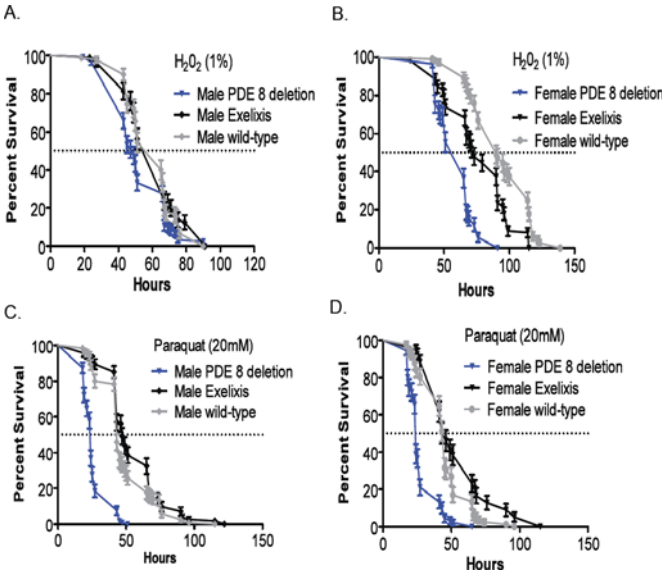

Fig. 8. – Silencing of PDE8 alters survival responses to oxidative stress in *Drosophila*. The survival rate of flies fed with 1% hydrogen peroxide is significantly reduced in (A) male PDE8 -deficient flies compared to the wild-type CantonS (p=0.0138; Log rank; Mantel-Cox) and Exilesis (p<0.0001) parents, and in (B) female (p<0.0001 against both controls). The survival rate of (C) male and (D) female fed with 20mM paraquat is significantly reduced in PDE8 - deficient flies compared to both control strain (p<0.0001; Log rank; Mantel-Cox).

previously by others as producing maximal impedance (35). Next we tested the effect of the disruptor peptide and control peptide on maximal cell index in HeLa cells produced following EGF treatment (Fig. 7B). The disruptor peptide clearly attenuated the maximal increase in cell index and this effect was mimicked by overexpression of the catalytically inactive (dominant negative) PDE8A construct in HeLa cells (Fig. 7C). These data suggest that integrity of the PDE8A-Raf-1 complex is crucial for maximal EGF signalling leading to morphological changes. These results agree well with the premise that PDE8A activity is integral for the regulation of Raf-1 dependent ERK signalling in HEK293 cells, and primary mouse Leydig cells (Fig. 6).

Using impedance based analysis, we also monitored the response of cells to stress, as loss of oxidative stress tolerance has been linked to the amplitude of the ERK signalling response (37). Treatment of HEK293 cells with either hydrogen peroxide or staurosporine caused a reduction of the cell viability to a value that was markedly enhanced by transfection of a dominant negative PDE8A construct (Figs. 7D and E). As hydrogen peroxide and staurosporine can also induce cell death, we assessed whether PDE8 plays a role in survival signalling. For this purpose we used *Drosophila melanogaster* as a model system. Indeed, we found that the disruption of the endogenous *PDE8* gene increased the sensitivity of flies to treatment with either hydrogen peroxide or paraquat. The survival rate of flies fed with 1% hydrogen peroxide was significantly reduced in male PDE8 -deficient flies compared to the wild-type CantonS and Exilesis parents (Fig. 8A), and in (Fig. 8B) female flies against both controls. The survival rate of male (Fig. 8C) and (Fig. 8D) female flies fed with 20mM paraquat is significantly reduced in PDE8 - deficient flies compared to both control strain. Thus, PDE8 function enhances survival, both at the cellular as well as the organism level.

DISCUSSION

Regulation of Raf activity is of pivotal important to the control of cell growth, survival and differentiation through the ERK signalling pathway (1). One important point of control is the

inhibitory phosphorylation of Raf-1 by PKA. However, to date the factors that influence this key regulatory event have been obscure. Here we identify a novel means of controlling this inhibitory process through sequestration of the cAMP hydrolysing PDE8A enzyme with Raf-1 itself. The importance of individual PDE families are becoming more appreciated, especially in the light of the bewildering complexity of PDE isoform expression and the often very specific biological effects of isoform selective PDE inhibitors (18). The cAMP effector, PKA can also bind to Raf-1 but, in contrast to PDE8A, the binding of PKA to Raf-1 is disrupted by cAMP agonists (4). Thus, PDE8A may function as a local, tonic antagonist of cAMP signalling, setting the threshold that needs to be overcome for Raf-1 activation. This view is consistent with our results, as we show that displacement of endogenous PDE8A by a catalytically inactive species generates a dominant negative phenotype (Figs 2 and 7). Additionally, the effects of a cell-permeable PDE8A disruptor peptide and genetic silencing of PDE8A to reduce the basal local PDE8A activity and subsequent increase in Raf-1 activation (Fig. 6) also adds weight to this proposal.

This identification of only the second binding partner for PDE8A (PDE8A also associates with IkappaB (49)) and of a PDE associated with Raf-1 strongly suggests that spatial regulation of Raf-1 can occur through sequestration of PDE8A. This may open new opportunities to manipulate Raf-1 activation by pharmacological agents that modulate PDE8A and for evaluating changes in this system in disease states. Raf-1 activation is now increasingly in the limelight as a promising drug target. While Raf-1 is rarely mutated in cancer (38), B-Raf is frequently mutated in melanoma (39), and the B-Raf selective inhibitor PLX4720 has shown impressive clinical efficacy in the treatment of B-Raf mutated melanomas (40). However, in melanomas with Ras mutations, these inhibitors were ineffective and even may cause tumour progression. The reason seems to be a paradoxical activation of ERK caused by the promotion of Raf-1 – B-Raf heterodimerization, which is stimulated by mutant Ras and Raf inhibitors (41, 42). The B-Raf – Raf-1 heterodimer has >30fold higher kinase activity than the respective homodimers or monomers, even when one of the two Raf kinases is inactivated (43). Thus, B-Raf despite being pharmacologically inhibited can recruit Raf-1 for signalling and efficient activation of the ERK pathway. In this context, PDE8A inhibitors should be beneficial and possibly synergistic with Raf inhibitors, as is shown here PDE8A inhibition can impede the activation of Raf-1. This hypothesis is supported by recent findings that melanocytes use B-Raf to activate ERK, as Raf-1 activity is suppressed by high cAMP levels (44). However, in response to Ras mutations occurring during melanoma development cells switch to use Raf-1 to activate the ERK pathway (44). This switch is promoted by mutant Ras stimulating a negative feedback phosphorylation of B-Raf by ERK, and an elevation of PDE4 activity. This shift de-inhibits Raf-1, and enables Raf-1 mediated oncogenic signalling. In fact, inhibiting Raf-1 by activating cAMP signalling blocks proliferation and induces apoptosis of Ras-mutated melanoma cells (45). Thus, PDE8A selective inhibitors may become important pharmacological agents to counteract oncogenic Raf signalling.

MATERIALS AND METHODS

Cell culture and transfection

HEK 293 and HeLa cells were cultured in Dulbecco's modified Eagle's medium supplemented with 10% fetal calf serum, 1% penicillin-streptomycin and 1% L-glutamine (all Sigma) at 37°C in humidified air with 5% CO_2. Transfections were performed using Polyfect (Qiagen) according to the manufacturer's instructions. Primary mouse Leydig cells were prepared and cultured from wild type and PDE8A (-/-) mice as previously described (22).

Mammalian cell expression constructs

Human Flag-tagged PDE8A1 in the pCMV-2 plasmid was a gift from Dr. Kenji Omori. The pEF-myc-Raf-1 construct was provided by Dr. Chris Marshall, and pGEX-KG-Raf-1 was described previously (10). For single transfections 8µg of DNA was used per 100mm plate, for dual transfections 4µg of each construct was transfected.

Chemicals and Antibodies

Forskolin, dipyridamole and 3-isobutyl-1-methylxanthine (IBMX) (Sigma) were dissolved in dimethyl sulfoxide (DMSO) and added to cell media at a concentration of <0.1% DMSO. Epidermal growth Factor (EGF), staurosporine, hydrogen peroxide were all obtained from Sigma. Antibodies against the myc tag (1:2000), phospho-ERK (1:1000), ERK (1:1000) and phospho-Raf-1 (pS259, 1:1000) were obtained from Cell Signaling. Raf-1 (1:2000) and PDE8A (1:2000) antibodies were purchased from BD Biosciences and Scottish Biomedical, respectively. HRP-conjugated Flag antibody (1:2000) was from Sigma and GST antibody (1:2000) from Santa Cruz.

Phosphodiesterase assay and cellular transfection of PDE8A1

Phosphodiesterase activity was measured using a radioactive cAMP hydrolysis assay that has been described previously (McCahill et al, 2005). [8-^{3}H] adenosine cyclic-3', 5'-mono-phosphate was from Amersham Biosciences (Little Chalfont, U.K.) and cyclic-3', 5'-mono-phosphate from Sigma. The substrate concentration used for PDE assays was 150 nM. Raf-1 immunoprecipitations were done from 400µg of cellular lysate.

MS analysis of Raf-1 immunoprecipitates

$1x10^7$ growing cells were lysed in PBS supplemented with 1% Triton X-100 and protease inhibitors (Complete protease inhibitor cocktail tablets, Roche) and phosphatase inhibitors (PhosSTOP tablets, Roche). Lysates were cleared by centrifugation (20,000g; 10 minutes) and the supernatant was immunoprecipitated with Raf-1 antibodies for 2 hours at 4°C. IPs were washed 3x in lysis buffer and separated on 7.5% SDS gels. Gels were stained with colloidal Coomassie stain (0.1% Coomassie R-250, 50% methanol, 5% acetic acid and 45% Milli-Q water) and destained in destaining solution (40% methanol, 10% acetic acid and 50% Milli-Q water) until the background was clear. Bands were cut out from the gel and chopped into ~ 1x1mm pieces. The gel pieces were washed with distilled water for 15 minutes, followed by two washes with 100 mM NH_4HCO_3 / CH_3CN (50:50 v/v) for 15 minutes. Then, gel pieces were crushed with a Teflon pestle, dehydrated in CH_3CN and dried in a Speedvac for 5 minutes. Gel pieces were incubated with 12.5 mg/ml of modified porcine trypsin (Promega) in 20 mM NH_4HCO_3 / 0.1% nOctyl-Glucoside at 30°C overnight. Then an equal volume of CH_3CN was added to the digest and incubated at 30°C for 30 minutes on a shaking platform. The digest supernatant was removed and dried down in a Speedvac. The digest was resuspended in 10 ml of 50% CH_3CN in 0.1% trifluoric acid and analysed on a VoyagerDE-Pro MALDI-TOF by peptide mass fingerprinting using 2,5-dihydroxy benzoic acid as matrix.

Western blotting

Cells were lysed in 3T3 lysis buffer (1% Triton X-100, 50 mM Hepes, pH 7.2, 10 mM EDTA and 100 mM $NaH_2PO_4 \cdot 2H_2O$) supplemented with protease inhibitors tablet (Roche). Detergent-insoluble proteins were removed by centrifugation at 10,000*g* for 10 minutes. Aliquots of the soluble fraction were resolved by sodium dodecyl sulphate poly acrylamide gel electrophoresis (SDS-PAGE) using the NuPAGE® system (Invitrogen, Carlsbad, CA 92008, USA). Proteins were transferred to nitrocellulose membrane (Protran®, Whatman GmbH, Hahnestraße 3, D-37586 Dassel, Germany) for 1 hour at 25V using NuPAGE® Transfer buffer. The membranes were blocked in 5% non-fat dry milk (marvel)/Tris-buffered saline supplemented with 0.1% Tween-20 (TBS-T) for at least 1 hour before primary antibodies were added in 1% marvel/TBS-T and incubated at 4°C overnight. The membranes were washed 3 times for 10 minutes in TBS-T. Peroxidase or Alexa-Fluor conjugated secondary antibodies were added in 1% marvel/TBST and incubated for 1 hour at room temperature. Membranes were washed as before, and bound primary antibodies were detected by incubation with appropriate secondary antibodies using either enhanced chemiluminescence (ECL) or the Licor Odyssey scanner for fluorescence detection. Densitometry on film was performed using Quantity One software (BioRad Laboratories, 1000 Alfred Nobel Drive, Hercules, CA 94547). Fluorescence intensity was measured using the Odyssey software (Licor). For ECL detection, the mouse (Amersham) and rabbit (Sigma) secondary antibodies were used at a 1:5000 concentration. The Odyssey secondary antibodies Alexa-Fluor® 680 and Alexa-Fluor® 800 were diluted 1:10,000.

Immunoprecipitation experiments (IPs)

Myc-Raf-1 and Flag-PDE8A1 were immunoprecipitated from 400-1000µg of total protein lysate made up to a total volume of 400µl with 3T3 lysis buffer using 50µl Myc (Sigma) or Flag (Invitrogen) antibodies coupled to agarose beads. The IPs were incubated for at least 2 hours or overnight at 4°C with constant agitation, before the beads were washed at least 3 times with 3T3 lysis buffer. For endogenous IPs, 10µg PDE8A antibody was incubated with 1000µg HeLa cell lysate overnight at 4°C with constant agitation. Washed protein G beads (Amersham) (75ul) were added for 1-2 hours before the beads were pelleted and washed as above.

Peptide Arrays

Peptide libraries were produced by automatic SPOT synthesis (46). They were synthesized on continuous cellulose membrane supports on Whatman 50 cellulose membranes using FMOC (9-fluorenylmethyloxycarbonyl) chemistry with the AutoSpot-Robot ASS 222 (Intavis Bioanalytical Instruments). The interaction of spotted peptides with GST and GST-Raf-1 was determined by overlaying the membranes with 10µg/ml recombinant protein. Bound

proteins were detected with GST antibody (Santa Cruz), and detection was performed with a secondary anti-rabbit antibody coupled with horseradish peroxidise (1:2500 dilution; Dianova) and ECL detection.

Disruptor peptides

All peptides were purchased from Genscript and dissolved in DMSO. The disruptor peptide (R454-T465) RRLSGNEYVLST was designed based on the peptide array results. The scrambled control peptide SYTVRLLGERNS sequence was created by randomly scrambling the disruptor peptide sequence, ensuring no vital residues were in the same position. To make them cell permeable, peptides were synthesized with a stearic acid group ($CH_3(CH_2)_{16}COOH$) attached to the C-terminus. Peptides were added to cells at a final concentration of 10μM for 4 hours before cells were harvested.

Site-directed mutagenesis

Site-directed mutagenesis was performed using the Quickchange kit (Stratagene). All primers were obtained from Thermo Scientific, and sequencing was performed by the DNA Sequencing Service at the University of Dundee. The following primers were used to create the required mutations:

R454A/R455A mutant:
Forward primer
5'-CTTAATGTCTGATGGTTTGGCGGCCCTATCAGGGAATGAATATGTTC-3'
Reverse primer
5'- GAACATATTCATTCCCTGATAGGGCCGCCAAACCATCAGACATTAAG -3'

E460A/Y461A mutant:
Forward primer
5'- CTATCAGGGGAATGCAGCTGTTCTTTCAACAAAAAACACTCAAATGG -3'
Reverse primer
5' – CCATTTGAGTGTTTTTTGTTGAAAGAACAGCTGCATTCCCTGATAG -3'

Both R454A/R455A and E461A/Y461A mutants were verified by sequencing using the F3 primer (see MBP-Cloning).

R454A/R455A/E460A/Y461A mutants:
Forward primer
5'–gggcttaatgtctgatggtttggcagcactatcagggaatgcagctgtt -3'
Reverse primer
5' – aacagctgcattccctgatagtgctgccaaaccatcagacattaagccc – 3'

PDE8A1 dominant negative D726A mutant:
Forward primer
5'-gctgattaaatgtgctgctgtgtccaatccctgcc-3'
Reverse primer
5'-ggcagggattggacacagcagcacatttaatcagc-3'

The D726A mutant was verified by sequencing using the CMV24 primer:
5' – GTGCCCACCAGCCTTGTCCTAATA – 3'

HEK293 cells overexpressing wt Flag-PDE8A1, D/N PDE8A1 and mock transfected were blotted for immunoreactivity and normalized to equal expression levels. The catalytic activity of D/N PDE8A1 versus wt PDE8A1 was measured by PDE assay as described elsewhere (47).

In vitro binding assay

Equimolar amounts (2μM) of purified recombinant GST (negative control) and GST-Raf-1 and PDE8A1 protein (Scottish Biomedical) were mixed in binding buffer (50mM Tris-HCl pH7.5, 100mM NaCl, 2mM $MgCl_2$, 1mM DTT, 0.5% (v/v) Triton X-100, 0.5% (w/v) BSA and protease inhibitors) and incubated for 1 hour at 4°C. 30μl of GST beads were washed and equilibrated in binding buffer, then added to the protein cocktail and incubated as before for 1 hour. Beads were sedimented by centrifugation at 10,000 x g for 1 minute, and washed 3 times. Proteins associated with the beads were eluted by boiling in sample buffer and analysed by Western blotting.

Surface plasmon resonance experiments

Surface Plasmon Resonance analysis was performed using a Biacore 2000 instrument (GE Healthcare). Anti-GST antibody (GST Capture Kit, GE Healthcare) was immobilized to a level of 15000 RU onto CM5 sensor chips (GE Healthcare) according to the manufacturer's instructions. The fusion protein GST-Raf-1 (100 nM) was reversibly captured to a level of 165-200 RU. As control surface an anti-GST surface captured with GST (1μg/ml) was prepared. The interaction study was performed in HBS buffer (20 mM Hepes pH 7.4, 150 mM NaCl and 0.01% surfactant Tween20) at 30 °C. Kinetic constants were determined by injecting a series of dilutions of MBP-PDE8A1 (900 nM – 3.5 nM) over GST-Raf-1 on the capture surfaces at a flow rate of 30 μl/min. The association was monitored for 5 min, whereas dissociation of the complex was followed for 60 min. Since less than 5% of the complex dissociates within 60 min, the dissociation time of the highest concentration (900nM) was prolonged to 480 min and used for quantification of the dissociation rate constant (k_d). After each interaction event, the antibody surface was regenerated using two pulses of 10 mM glycine (pH 1.7). Data were evaluated using the software BIAevaluation 4.1 (GE Healtchcare) and Graphpad Prism 5.04 (GraphPad Software Inc., La Jolla, CA, USA). Kinetic rate constants (k_a and k_d) were determined by simultaneously fitting experimental data to rate equations derived from a Langmuir 1:1 binding model. As k_d can only be determined accurately, if at least 5% of bound material dissociates, the upper limit of k_d has been calculated using the equation $k_d = -\ln(0.95)/td$, where td is time (in seconds) allowed for dissociation. Sensorgrams were double referenced using the control surface (GST) and blank buffer injections to subtract baseline drifts from the data sets. To assess reproducibility of kinetic constants the analysis was performed in duplicate.

To test whether the interaction between PDE8A1 and Raf-1 is inhibited by a selective PDE8 inhibitor, MBP-PDE8A1 (100 nM) was pre-incubated with 50 μM Dipyrimidole and injected over GST-Raf-1 on the capture surfaces. The binding mode of Dipyrimidole and GST-Raf-1 was tested separately in a control experiment.

To generate the MBP-PDE8A1 bacterial expression vector the Flag-PDE8A1 construct was used as a template to amplify the PDE8A1 insert and incorporate the *SalI* and *XbaI* recognition sites by PCR using the following primers.

Forward primer: 5' – AATCTAGAATGGGCTGTGCCCCGA – 3'
Reverse primer: 5' – AAGTCGACCTATTCAGGAGGTGGTC – 3'

The PCR product and pMAL-c2x vector (NEB) were digested using *XbaI* and *SalI* restriction enzymes and ligated. The construct was sequenced using the following primers:

Forward 1 primer: 5' -GATGAAGCCCTGAAAGACGCGCAG – 3'
Reverse 1 primer: 5' - GAT TTA ATC TGT ATC AGG – 3'
Forward 2 primer: 5' -GAA GAG TTG TCC GTA ATG -3'
Reverse 2 primer : 5' - GCA GGG ATT GGA CAC ATC – 3'
Forward 3 primer: 5' - ATA TCC GAA TGT GTT CAG – 3'
Reverse 3 primer: 5' - CAC ATC AGC AGA ATG TGT – 3'

To purify Raf-1 and PDE8A1 proteins for the SPR experiments a 10 ml overnight culture of BL21 *E.coli* cells containing the pGEX-GST-Raf-1 or pMAL-c2x plasmids was added to 500ml of LB medium and grown at 37°C with shaking until the OD_{600} reached approximately 0.6. Expression of the recombinant fusion proteins was induced by adding 0.1mM isopropyl-β-D-1-thiogalactopyranoside (IPTG). After 4 hours cells were pelleted by centrifugation at 7,000xg for 7 minutes and frozen at -80°C to assist with lysis. The bacterial pellet was lysed as described (48), and fusion proteins were isolated by incubating the lysates with either glutathione sepharose beads or amylose resin (Amersham) for one hour at 4°C. Beads were washed 6-8 times in PBS and the fusion proteins were released by incubating with 600μl of elution buffer (10 mM of glutathione in 50mM of Tris, pH 7.5 or 50mM maltose) for 20 minutes at 4°C. The elution step was repeated 3 times and the eluates were pooled. Any detergent, glutathione or maltose was removed by overnight dialysis using the slide-a-lyzer cassettes (Piercenet) in 2 litres of dialysis buffer.

Measuring cellular responses with the xCELLigence system

The E-Plate 96 (Roche) was used for these experiments as previously described by us {Anthony, #27}. This comprises a 96-well plate with integral sensor electrode arrays to measure cell impedance. The xCELLigence system was used according to the instructions of the supplier (Roche Applied Science). The E-plate 96 is a single use, disposable 96-well microtiter plate used for performing cell-based assays on the RTCA SP instrument. It has incorporated gold cell sensor arrays in the bottom, which allows impedance inside each well to be monitored and assayed in real time. The impedance is reported as arbitary cell index measurements. HeLa cells were transfected with D/N PDE8A and 24 hours later seeded onto a 96 well E-plate (Roche) at a density of 2 x 10^4 cells per well. Cells were allowed to adhere overnight before any treatment. For disruptor peptide experiments, cells were treated with the peptides for 4 hours before further treatment. Then, cells were serum starved for 4 hours before treatment with 100 ng/ml EGF. After treatment, the cell index was measured every 15 seconds using the xCELLigence system (Roche). For measuring cell death after treatment with staurosporine 500 nM or hydrogen peroxide 10 μM, HEK293 cells were plated as above and the cell index was measured every 30 minutes. Cell viability was measured by calculating the cell index of treated cells as a percentage of non-treated cells.

Generation of the PDE8 deletion in Drosophila

The *Drosophila* PDE8 deletion was generated using FLP recombinase and two lines containing FRT-bearing *piggybac* insertions. The *piggybac* insertions lines ($PDE8^{d06642}$ and $PDE8^{f02577}$) flank most of the PDE8 coding region including the entire catalytic domain. Individual lines were screened with PCR of genomic DNA to confirm the loss of the intervening DNA.

Drosophila survival assays in response to oxidative stress

5-7 day old flies of specified genotype (males and females housed separately) were starved for 4 h and then exposed to either 20 mM paraquat or 1% H_2O_2 (All Sigma) in 1% sucrose media in groups of 30, with three biological replicates. Flies were counted until 100% mortality was reached and data expressed as % survival ± SEM (N = 3). Data were assessed for significance by the LogRank (Mantel-Cox) test using Graph Pad Prism 5.0 software.

Whole flies phospho-ERK western blot analysis

Basal phospho-ERK levels were analyzed from PDE8 deficient flies compared with two control strains, wild-type CantonS flies and Exilexis flies, to control for genetic background of PDE8 deficient line. Briefly, 50 flies of each genotype were washed and gently homogenized in ice-cold 3T3 lysis buffer supplemented with 1:100 dilution of protease-inhibitor cocktail (Sigma) using an eppendorf micropestle. The homogenate was then subjected to two successive centrifugations at 1000 x g at 4 °C for 5 min to remove large cuticle debris and wings, and protein concentration was determined using Bio-Rad Bradford assay

ACKNOWLEDGEMENTS.

GSB, KB, MDH, JPD and FC were supported by the Medical Research Council (UK; G0600765) and Fondation Leducq (06CVD02). This work was supported by the Science Foundation Ireland under Grant No. 06/CE/B1129 for WK and DR. This work was supported by the European Union Sixth Framework Programme specific targeted project thera-cAMP (Contract 037189) and the Seventh Framework Programme collaborative project AffinityProteome (Contract 222635) for BZ and KH. NIH grant NS29740 (DBM) and GM083926 JAB), Biotechnological and Biological Sciences Research Council (UK) grant BB/G020620/1 (S-A.D)

1. Yoon S & Seger R (2006) The extracellular signal-regulated kinase: multiple substrates regulate diverse cellular functions. *Growth Factors* 24(1):21-44
2. Kubicek M, *et al.* (2002) Dephosphorylation of Ser-259 regulates Raf-1 membrane association. *J Biol Chem* 277(10):7913-7919.
3. Jaumot M & Hancock JF (2001) Protein phosphatases 1 and 2A promote Raf-1 activation by regulating 14-3-3 interactions. *Oncogene* 20(30):3949-3958.
4. Dumaz N & Marais R (2003) Protein kinase A blocks Raf-1 activity by stimulating 14-3-3 binding and blocking Raf-1 interaction with Ras. *J Biol Chem* 278(32):29819-29823.
5. Dhillon AS, *et al.* (2002) Cyclic AMP-dependent kinase regulates Raf-1 kinase mainly by phosphorylation of serine 259. *Mol Cell Biol* 22(10):3237-3246 .
6. Sutherland EW & Robison GA (1966) The role of cyclic-3',5'-AMP in responses to catecholamines and other hormones. *Pharmacol Rev* 18(1):145-161 .
7. Walsh DA, *et al.* (1972) Cyclic AMP-dependent protein kinases from skeletal muscle and liver. *Adv Cyclic Nucleotide Res* 1:33-45 .
8. Cook SJ & McCormick F (1993) Inhibition by cAMP of Ras-dependent activation of Raf. *Science* 262(5136):1069-1072 .
9. Burgering BM, Pronk GJ, van Weeren PC, Chardin P, & Bos JL (1993) cAMP antagonizes p21ras-directed activation of extracellular signal-regulated kinase 2 and phosphorylation of mSos nucleotide exchange factor. *EMBO J* 12(11):4211-4220 .
10. Hafner S, *et al.* (1994) Mechanism of inhibition of Raf-1 by protein kinase A. *Mol Cell Biol* 14(10):6696-6703 .
11. Sevetson BR, Kong X, & Lawrence JC, Jr. (1993) Increasing cAMP attenuates activation of mitogen-activated protein kinase. *Proc Natl Acad Sci U S A* 90(21):10305-10309 .
12. Graves LM, *et al.* (1993) Protein kinase A antagonizes platelet-derived growth factor-induced signaling by mitogen-activated protein kinase in human arterial smooth muscle cells. *Proc Natl Acad Sci U S A* 90(21):10300-10304 .
13. Wu J, *et al.* (1993) Inhibition of the EGF-activated MAP kinase signaling pathway by adenosine 3',5'-monophosphate. *Science* 262(5136):1065-1069 .
14. Matallanas D, *et al.* (2011) Raf family kinases: old dogs have learned new tricks. *Genes Cancer* 2(3):232-260 .
15. Gerits N, Kostenko S, Shiryaev A, Johannessen M, & Moens U (2008) Relations between the mitogen-activated protein kinase and the cAMP-dependent protein kinase pathways: comradeship and hostility. *Cell Signal* 20(9):1592-1607 .
16. Houslay MD & Kolch W (2000) Cell-type specific integration of cross-talk between extracellular signal-regulated kinase and cAMP signaling. *Mol Pharmacol* 58(4):659-668 .
17. Conti M & Beavo J (2007) Biochemistry and physiology of cyclic nucleotide phosphodiesterases: essential components in cyclic nucleotide signaling. *Annu Rev Biochem* 76:481-511 .
18. Houslay MD (2009) Underpinning compartmentalised cAMP signalling through targeted cAMP breakdown. *Trends Biochem Sci* 35(2):91-100 .
19. Baillie GS (2009) Compartmentalized signalling: spatial regulation of cAMP by the action of compartmentalized phosphodiesterases. *FEBS J* 276(7):1790-1799 .
20. Zaccolo M (2011) Spatial control of cAMP signalling in health and disease. *Curr Opin Pharmacol* 11(6):649-655 .
21. Wang H, *et al.* (2008) Kinetic and structural studies of phosphodiesterase-8A and implication on the inhibitor selectivity. *Biochemistry* 47(48):12760-12768 .
22. Vasta V, Shimizu-Albergine M, & Beavo JA (2006) Modulation of Leydig cell function by cyclic nucleotide phosphodiesterase 8A. *Proc Natl Acad Sci U S A* 103(52):19925-19930 .
23. Vang AG, *et al.* (2010) PDE8 regulates rapid Teff cell adhesion and proliferation independent of ICER. *PLoS One* 5(8):e12011 .
24. Dong H, Osmanova V, Epstein PM, & Brocke S (2006) Phosphodiesterase 8 (PDE8) regulates chemotaxis of activated lymphocytes. *Biochem Biophys Res Commun* 345(2):713-719 .
25. Patrucco E, Albergine MS, Santana LF, & Beavo JA (2010) Phosphodiesterase 8A (PDE8A) regulates excitation-contraction coupling in ventricular myocytes. *J Mol Cell Cardiol* 49(2):330-333 .
26. Soderling SH, Bayuga SJ, & Beavo JA (1998) Cloning and characterization of a cAMP-specific cyclic nucleotide phosphodiesterase. *Proc Natl Acad Sci U S A* 95(15):8991-8996 .
27. Baillie GS, *et al.* (2007) Mapping binding sites for the PDE4D5 cAMP-specific phosphodiesterase to the N- and C-domains of beta-arrestin using spot-immobilized peptide arrays. *Biochem J* 404(1):71-80 .
28. Meng D, *et al.* (2009) MEK1 binds directly to betaarrestin1, influencing both its phosphorylation by ERK and the timing of its isoprenaline-stimulated internalization. *J Biol Chem* 284(17):11425-11435 .
29. Anthony DF, *et al.* (2011) beta-Arrestin 1 inhibits the GTPase-activating protein function of ARHGAP21, promoting activation of RhoA following angiotensin II type 1A receptor stimulation. *Mol Cell Biol* 31(5):1066-1075 .
30. Bjorgo E, *et al.* (20100Cross talk between phosphatidylinositol 3-kinase and cyclic AMP (cAMP)-protein kinase a signaling pathways at the level of a protein kinase B/beta-arrestin/cAMP phosphodiesterase 4 complex. *Mol Cell Biol* 30(7):1660-1672 .
31. Perino A, *et al.* (2011) Integrating cardiac PIP3 and cAMP signaling through a PKA anchoring function of p110gamma. *Mol Cell* 42(1):84-95 .
32. Smith KJ, *et al.* (2007) 1H NMR structural and functional characterisation of a cAMP-specific phosphodiesterase-4D5 (PDE4D5) N-terminal region peptide that disrupts PDE4D5 interaction with the signalling scaffold proteins, beta-arrestin and RACK1. *Cell Signal* 19(12):2612-2624 .
33. Rampersad SN, *et al.* (2010) Cyclic AMP phosphodiesterase 4D (PDE4D) Tethers EPAC1 in a vascular endothelial cadherin (VE-Cad)-based signaling complex and controls cAMP-mediated vascular permeability. *J Biol Chem* 285(44):33614-33622 .
34. Friedman AA, *et al.* (2011) Proteomic and functional genomic landscape of receptor tyrosine kinase and ras to extracellular signal-regulated kinase signaling. *Sci Signal* 4(196):rs10 .
35. Atienza JM, *et al.* (2006) Dynamic and label-free cell-based assays using the real-time cell electronic sensing system. *Assay Drug Dev Technol* 4(5):597-607 .
36. Starsichova A, *et al.* (2009) Dynamic Monitoring of Cellular Remodeling Induced by the Transforming Growth Factor-beta1. *Biol Proced Online* 11:316-324 .
37. Ikeyama S, Kokkonen G, Shack S, Wang XT, & Holbrook NJ (2002) Loss in oxidative stress tolerance with aging linked to reduced extracellular signal-regulated kinase and Akt kinase activities. *FASEB J* 16(1):114-116 .
38. Zebisch A & Troppmair J (2006) Back to the roots: the remarkable RAF oncogene story. *Cell Mol Life Sci* 63(11):1314-1330 .
39. Davies H, *et al.* (2002) Mutations of the BRAF gene in human cancer. *Nature* 417(6892):949-954 .
40. Flaherty KT, *et al.* (2010) Inhibition of mutated, activated BRAF in metastatic melanoma. *N Engl J Med* 363(9):809-819 .
41. Poulikakos PI, Zhang C, Bollag G, Shokat KM, & Rosen N (2010) RAF inhibitors transactivate RAF dimers and ERK signalling in cells with wild-type BRAF. *Nature* 464(7287):427-430 .
42. Heidorn SJ, *et al.* (2010) Kinase-dead BRAF and oncogenic RAS cooperate to drive tumor progression through CRAF. *Cell* 140(2):209-221 .
43. Rushworth LK, Hindley AD, O'Neill E, & Kolch W (2006) Regulation and role of Raf-1/B-Raf heterodimerization. *Mol Cell Biol* 26(6):2262-2272 .
44. Dumaz N, et al. (2006) In melanoma, RAS mutations are accompanied by switching signaling from BRAF to CRAF and disrupted cyclic AMP signaling. Cancer Res 66(19):9483-9491 .
45. Marquette A, Andre J, Bagot M, Bensussan A, & Dumaz N (2011) ERK and PDE4 cooperate to induce RAF isoform switching in melanoma. Nat Struct Mol Biol 18(5):584-591 .
46. Kramer A & Schneider-Mergener J (1998) Synthesis and screening of peptide libraries on continuous cellulose membrane supports. Methods in Molecular Biology; Combinatorial peptide library protocols, Methods in Molecular Biology : 87, (Humana Press Inc.), pp 25-39.
47. McCahill A, et al. (2005) In resting COS1 cells a dominant negative approach shows that specific, anchored PDE4 cAMP phosphodiesterase isoforms gate the activation, by basal cyclic AMP production, of AKAP-tethered protein kinase - A type II located in the centrosomal region. Cell. Signal. 17(9):1158-1173.
48. Frangioni JV & Neel BG (1993) Solubilization and Purification of Enzymatically Active Glutathione-S-Transferase (Pgex) Fusion Proteins. Anal. Biochem. 210(1):179-187.
49. Wu P & Wang P (2004) Per-Arnt-Sim domain-dependent association of cAMP-phosphodiesterase 8A1 with IkappaB proteins. *Proc Natl Acad Sci U S A* 101(51):17634-17639 .